Implementation of the CRPA model in the GENIE event generator and analysis of nuclear effects in low-energy transfer neutrino-nucleus interactions

S. Dolan,[1] A. Nikolakopoulos,[2] O. Page,[3] S. Gardiner,[4] N. Jachowicz,[2] and V. Pandey[5]

[1] *CERN, European Organization for Nuclear Research, Geneva, Switzerland*[*]
[2] *Department of Physics and Astronomy, Ghent University, Proeftuinstraat 86, B-9000 Gent, Belgium*[†]
[3] *School of Physics, University of Bristol, Bristol BS8 1TL, United Kingdom*
[4] *Fermi National Acclerator Laboratory, Batavia, IL 60502, USA*
[5] *Department of Physics, University of Florida, Gainesville, FL 32611, USA*[‡]

(Dated: October 28, 2021)

We present the implementation and validation of the Hartree-Fock continuum random phase approximation (HF-CRPA) model in the GENIE neutrino-nucleus interaction event generator and a comparison of the subsequent predictions to experimental measurements of lepton kinematics from interactions with no mesons in the final sate. These predictions are also compared to those of other models available in GENIE. It is shown that, with respect to these models, HF-CRPA predicts a significantly different evolution of the cross section when moving between different interactions targets, when considering incoming anti-neutrinos compared to neutrinos and when changing neutrino energies. These differences are most apparent for interactions with low energy and momentum transfer. It is also clear that the impact of nucleon correlations within the HF-CRPA framework is very different than in GENIE's standard implementation of RPA corrections. Since many neutrino oscillation experiments rely on their input model to extrapolate between targets, flavours, and neutrino energies, the newly implemented HF-CRPA model provides a useful means to verify that such differences between models are appropriately covered in oscillation analysis systematic error budgets.

I. INTRODUCTION

Whilst accelerator-based neutrino oscillation experiments such as T2K [1], NOvA [2], Hyper-K [3] and DUNE [4], offer an unprecedented opportunity to explore fundamental physics, such as the neutrino mass ordering and Charge-Parity violation (CPV) in the lepton sector, their success relies on a detailed understanding of sub-to-few-GeV neutrino-nucleus interactions. Unfortunately, no existing interaction model is able to quantitatively describe available data, necessitating the application of large systematic uncertainties in model predictions [5]. The impact of these uncertainties on neutrino oscillation analyses is often mitigated through the use of a "near" detector, which is exposed to the unoscillated neutrino beam, to constrain the uncertainties on the oscillated event rate at a "far" detector. However, a neutrino interaction model is still usually required to extrapolate between the different neutrino energies, beam flavour compositions, kinematic acceptances and sometimes different target materials of the near and far detectors. It is equally crucial that models are able to reliably predict the asymmetry between neutrino and anti-neutrino cross sections, such that these differences are not mistaken for a source of CPV. It is therefore important that systematic uncertainties on neutrino interaction models are able to reliably cover the plausible variation of differences in neutrino interaction cross sections between neutrino energies, flavours, kinematics and targets.

It has previously been shown that the Hartree-Fock (HF) mean-field model for charged-current quasi-elastic (CCQE) interactions with continuum random phase approximation (CRPA) corrections, developed by the Ghent group [6, 7], is successful in describing inclusive electron scattering data and predicts significantly different cross sections at low energy transfer compared to more widely used Fermi-gas models [8]. The CRPA corrections account for long-range correlations through a framework with an effective Skyrme nucleon-nucleon two-body interaction [9, 10]. It is particularly interesting to note that the treatment of final state interactions (FSI) via a distortion of the outgoing nucleon wave function within the HF-CRPA model leads to significantly different predictions for muon and electron neutrino cross sections at low energy transfers compared to widely used plane wave impulse approximation (PWIA) models (which do not include FSI) [11]. In this paper we report the implementation of the HF-CRPA model in the GENIEv3 neutrino-nucleus interaction event generator [12, 13] and evaluate how else it differs from other available CCQE models. Particular focus is placed on how the predictions differ between different nuclear targets and between neutrino and anti-neutrino interactions within the low energy and momentum transfer region where nuclear effects are most relevant.

The predictions from the HF-CRPA model are compared to those of SuSAv2 [14, 15] (implemented in GENIE in Ref. [16]) as well as the Valencia group's Local Fermi Gas (LFG) model [17] with and without RPA corrections to account for nucleon correlations. The models

* Contact e-mail: Stephen.Joseph.Dolan@cern.ch
† Contact e-mail: Alexis.Nikolakopoulos@UGent.be
‡ Present Address: Fermi National Accelerator Laboratory, Batavia, Illinois 60510, USA

This manuscript has been authored by Fermi Research Alliance, LLC under Contract No. DE-AC02-07CH11359 with the U.S. Department of Energy, Office of Science, Office of High Energy Physics.

are also compared to data provided by two T2K measurements reporting the cross section of charged current meson-less (CC0π) final states from interactions on carbon and oxygen targets [18] for incoming neutrinos and anti-neutrinos [19]. To make a complete comparison, a 2-particle 2-hole (2p2h) and pion absorption contribution must be added to the CCQE predictions. In all cases the SuSAv2 MEC model [20, 21] is used for 2p2h. For other channels the models of GENIE configuration `G18_10b` are used, containing the Berger-Seghal single pion production [22] model in addition to more inelastic channels fed through the "hN" intranuclear cascade model [23] to predict possible meson-less final states.

The paper is structured to first show the implementation scheme of the HF-CRPA model in Sec. II. A broad comparison of inclusive model predictions is then made in Sec. III, including comparisons of the models to T2K measurements. Conclusions are drawn in Sec. IV.

II. IMPLEMENTATION SCHEME

The implementation of neutrino interaction models in neutrino event generators requires a fast method of calculating the differential cross section given some set of outgoing particle kinematics (as are typically proposed via standard rejection sampling methods). In order for the implemented model to exactly reflect the microscopic theory on which it is based, the cross section would need to be available as a function of the set of kinematics to describe the entire final state (i.e. the fully *exclusive* cross section must be calculable). For the case of a CCQE interaction (neglecting any additional nuclear emission from FSI), this would require the calculation of the five-dimensional differential cross section as a function of the outgoing lepton and nucleon kinematics. However, few microscopic models are able to reliably provide such exclusive cross sections without relying on the factorized form implied by the PWIA (and none that can are currently implemented in neutrino event generators). Many models, such as e.g. the SuSAv2 approach, are specifically designed to provide *inclusive* cross sections, yielding results as function of the outgoing lepton kinematics only. Such models can be implemented in generators using a "factorisation approach" (as detailed in [16]) in which the lepton kinematics are calculated directly from a microscopic model calculation, before the hadronic system is added on top using approximate methods. For CCQE interactions this typically involves sampling a nucleon momentum and removal energy from some input spectral function, transferring it the appropriate four-momentum derived from the incoming neutrino energy and outgoing lepton kinematics, and then putting the resultant nucleon through a semi-classical FSI cascade model. Such an approach generally relies on the assumption that the nuclear ground state "seen" by the interaction is independent of the interaction's kinematics (although to partially alleviate this it is possible to make the sampled spectral function depend on the four momentum transfer). The resultant model can be seen to provide a fully accurate reflection of the microscopic models predictions for lepton kinematics but only a broad estimation for outgoing hadron kinematics given the information available. The HF-CRPA model that is the subject of this work is not explicitly limited to the calculation of inclusive observables, instead the energy and angle of the outgoing nucleon are obtained through a multipole decomposition [9, 10]. One is still faced with the fact that, due to the presence of FSI in the distorted wave treatment, and further due to the RPA, the exclusive cross section does not factorise as in the PWIA. Retaining the full complexity of the model would thus require sampling in a higher-dimensional phase space, making the process inefficient. In the present work we hence only include the cross section in terms of lepton kinematics, by summing and integrating over the outgoing nucleon's energy and angle. The effect of the approximations made in the factorised approach described below can, in future work, be compared to a more complete implementation of the kinematic degrees of freedom, using for example the approach described in [24]. This falls out of the scope of the present work however, where only the description of inclusive cross sections are considered.

The "factorisation approach" implementation scheme used to add HF-CRPA to GENIE is very similar to that used for the SuSAv2 CCQE model. The scheme benefits from the fact that the differential cross section can be written as the product of kinematic factors with the contraction of a generic lepton tensor and a model-specific hadron tensor, where the latter encodes all of the nuclear dynamics of the interaction. In this way, the implementation of HF-CRPA is achieved by inserting new hadron tensor look-up tables into GENIE (as previously done in [16, 25]). Separate tensors are provided for HF with and without CRPA corrections and for carbon, oxygen and argon targets. Separate tables are provided for the charged-current neutrino and anti-neutrino interactions, which is a necessity for describing the cross section on asymmetric nuclei such as Argon. Small isospin breaking effects are present in the responses even in the case of the even-even nuclei. These are due to the Coulomb potential of the nucleus which leads to differences in the binding energy of protons and neutrons in the initial state, but is also included consistently in the final-state for interactions in which a proton is emitted [26]. The responses can be further separated into their vector-vector, axial-axial, and vector-axial contributions. This separation makes it possible to consistently modify the axial form factor based on a single table by simply rescaling the axial-axial and vector-axial contributions. To predict cross sections for targets which do not have tables a simple "scaling of the second kind" is assumed [27, 28], extrapolating from the closest available tensor and accounting for the shift in the Fermi momentum between targets alongside an offset in the nuclear removal energy.

The HF-CRPA model is especially well-suited to cap-

ture the non-trivial nuclear effects that manifest themselves at small energy and momentum transfers, for example the presence of giant-resonances. A non-uniform binning scheme for the hadron tables is therefore used to capture the details of the model at low energy transfers, where the cross section evolves rapidly for fixed incoming neutrino energy due to such resonances. The nuclear response obtained in HF-CRPA naturally evolves from this low-energy region into a robust description of the quasielastic regime up to intermediate momentum transfers [7]. As the model is non-relativistic however, its reliability decreases with increasingly large momentum transfers. For the description of the nuclear response in this region, other approaches should be found more suitable. The HF-CRPA cross section is found to give very similar results to fully relativistic calculations in the region of intermediate momentum transfers where both the relativistic and non-relativistic approaches are found to be applicable [29]. This means that it should be possible to provide a description for the whole phase space by smoothly transitioning to a high-energy model in the region of intermediate momentum transfer, thereby retaining the detailed description of nuclear effects in the low-energy region while curing the ailments of non-relativistic approaches a high energy transfers.

To achieve this, the implementation provides tables up to 1 GeV energy transfer, but then supports the option to interpolate between the responses calculated by HF(-CRPA) and SuSAv2. In this manuscript a linear interpolation is employed between fully HF(-CRPA) and fully SuSAv2 in the region of 500 MeV to 1 GeV q_0. This is relevant for only a small portion of the total cross section, the interpolated model predicts that 7% (<1%) of the T2K flux integrated cross section has q_0>500 MeV(>1 GeV). Fig. 1 shows SuSAv2 and HF-CRPA cross sections with and without the extension, demonstrating its almost negligible role at intermediate kinematics, only becoming impactful close to and beyond the range of validity of the implemented HF-CRPA tables. A more cautious treatment of the interpolation may be required with larger incoming neutrino energies for analyses focused in the high energy transfer region. For example, for 2 GeV incoming neutrino energy the interpolated model predicts that 26% (5%) of the cross section has q_0>500 MeV(>1 GeV).

The hadron kinematics are calculated using identical methods to the SuSAv2 implementation, using a local Fermi gas spectral function with a custom momentum-transfer dependent removal energy derived from relativistic mean field model predictions [14, 16, 28, 30]. Validations of the model implementation are detailed and shown in Appendix A.

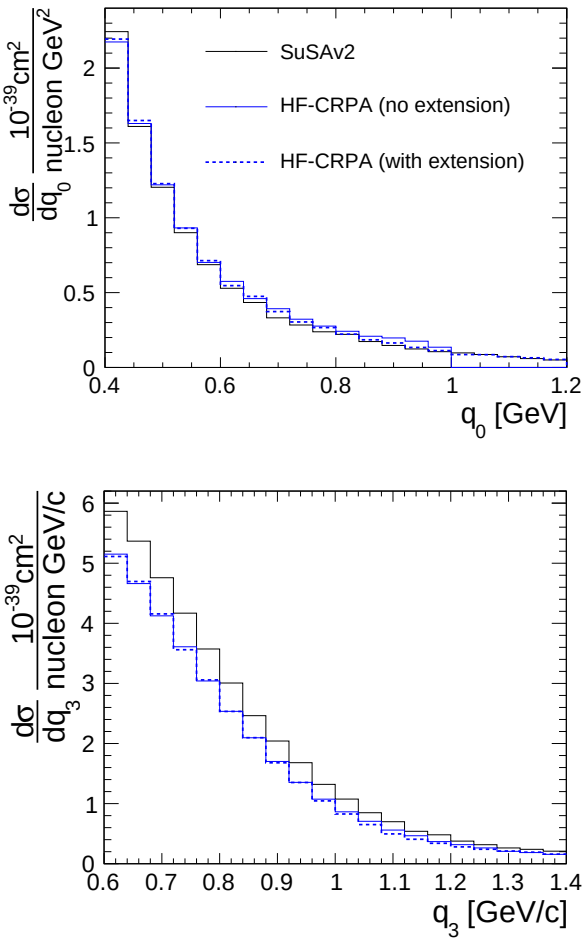

FIG. 1. A demonstration of the model extension employed at high q_0 between the HF-CRPA and SuSAv2 models. The single-differential T2K flux integrated cross section in the tails of q_0 and q_3 are shown (where the extension is most relevant) alongside the predictions of SuSAv2 and HF-CRPA before and after the high q_0 extension as calculated by GENIE. The small differences between HF-CRPA with and without the correction at q_0 below 500 MeV are from statistical variations in the GENIE Monte-Carlo simulation.

III. COMPARISON OF CRPA WITH OTHER MODELS IN GENIE

The evolution of the neutrino and anti-neutrino cross sections as a function of neutrino energy for HF-CRPA as well as the other considered GENIE CCQE models are shown in Fig. 2, while the double differential cross section as a function of energy (q_0) and momentum (q_3) transfer integrated over the T2K flux [31, 32] is shown in Fig. 3. Note that the nucleon axial mass parameter within all models is set to between 0.99 GeV and 1.03 GeV. The cross section suppression from CRPA and RPA is clear in both figures, although it can be seen that the shape of the suppression and the differences in the neutrino and anti-

neutrino cases are quite different. It should be noted that the physics content of an RPA approach is determined by the residual interaction and the mean-field propagator, which are significantly different in the LFG-RPA and and HF-CRPA approaches as discussed e.g. in [33].

In general the suppression from RPA in the Valencia group's LFG model is concentrated at low q_3 and causes a small enhancement of the cross section at larger q_0, q_3. CRPA instead causes very little enhancement of the cross section and its suppression is generally significantly weaker. It can also be noted that CRPA's suppression acts most strongly at slightly higher q_0 compared to the RPA case and extends to larger q_0, q_3. Fig. 3 additionally demonstrates that the GENIE implementation of the Valencia LFG model is restricted to producing events within a limited kinematic phase-space close to the peak region, whilst HF-CRPA is not.

The tighter region in which RPA impacts GENIE's LFG model also manifests as a much stronger suppression than that caused by CRPA on top of HF at low neutrino energy (before the cross section saturates and so when the low q_0, q_3 is responsible for a larger portion of the cross section). Since anti-neutrino interactions favour forward scattering, the impact of RPA continues to act as a significant suppression up to larger anti-neutrino energies. In general the relative size of the suppression is larger for CRPA at higher neutrino energies and for RPA at lower neutrino energies.

The large suppression found in HF-CRPA compared to HF, should be interpreted as a lower bound in this work. The HF-CRPA calculations provide a consistent treatment of long-range correlations beyond the HF mean field by using the same nucleon-nucleon interaction used to generate the HF mean field as residual interaction in the RPA. This interaction has to be regularized at large energy-momentum transfers, which was done through dipole form factor determined from a global fit to inclusive electron scattering data over a large kinematic range [7]. In Refs. [26, 34] it was noted that in particular kinematic regions, for relatively small energy and momentum transfer, this cut-off can be too strong and electron scattering data tends to be described well if the full strength of the residual interaction is retained. Following the results presented in Ref. [26], we do not include this effect in the present calculations for T2K kinematics, and for T2K flux-averaged cross section the HF and CRPA calculations can be considered as an upper and lower bound. We have however included tables which implement the dipole cutoff determined in [7] as it is a more suitable approach if higher-energy cross sections are considered.

A. Analysis of T2K measurements

As described in Sec. I, each model is extended from CCQE-only to CC0π by adding a SuSAv2 2p2h and a standard GENIE pion absorption components such that they can be compared to model independent experimental data (a very small CCQE contribution is also removed due to pion production FSI). In view of exploring model differences between different nuclear targets and flavours, the models are compared to T2K measurements of the CC0π cross section made simultaneously for either carbon and oxygen targets [18] or for neutrinos and anti-neutrinos [19]. The ability for each model to describe the data is shown as a χ^2 score calculated using the full experimental covariance matrix in Tab. I. Note that all the plots shown do not include all experimental bins. Very high momentum bins with large uncertainties in both measurements are not shown and for the neutrino and anti-neutrino case in Sec. III A 2 some of the high angle slices are also not shown since the focus of the discussion concerns the more forward angular region. The χ^2 score includes all bins.

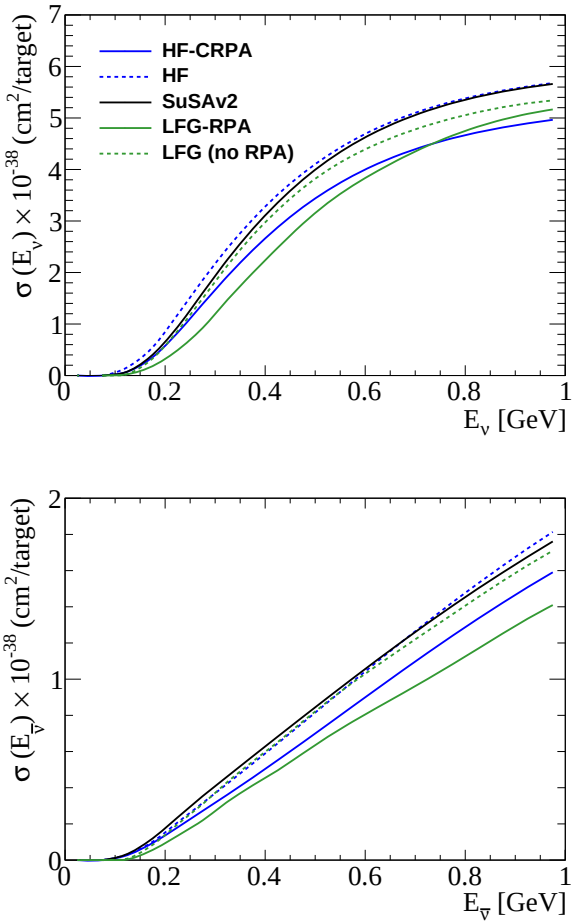

FIG. 2. The evolution of the total CCQE cross section on carbon predicted by various models as a function of neutrino energy is shown for neutrino and anti-neutrino cross sections in the upper and lower plot respectively. Note that, as detailed in the text, the large suppression found in HF-CRPA compared to HF should be interpreted as a lower bound in this work.

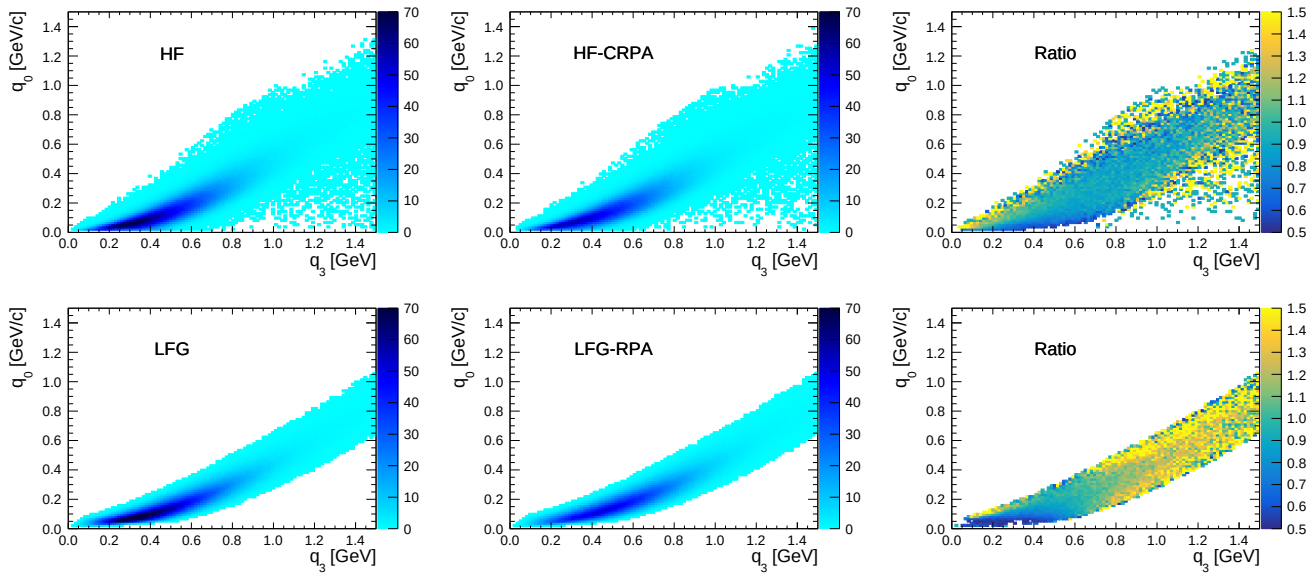

FIG. 3. The left and centre T2K muon neutrino flux (peaking at 0.6 GeV) averaged double differential cross section on carbon as a function of the energy (q_0) and momentum transfer (q_3) shown (on the z-axis) 10^{-39} cm^2 GeV^{-2}/c per nucleon with and without (C)RPA corrections. All plots are produced with GENIE. The plot on the right shows the impact of the corrections as a ratio. The upper row shows predictions from HF(-CRPA) model whilst the the lower row shows the same for the Valencia LFG(+RPA) model. White regions indicate regions in which no events were generated.

	Carbon and oxygen	ν_μ and $\bar{\nu}_\mu$
Number of bins	58	116
HF-CRPA	131.6	658.2
HF	183.0	817.9
SuSAv2	140.3	741.0
LFG-RPA	58.5	445.7
LFG (no RPA)	184.1	1027.5

TABLE I. The χ^2 calculated from comparing each model to T2K ν_μ CC0π cross section measurements jointly on carbon and oxygen targets [18] or for neutrinos and anti-neutrinos [19] interactions on hydrocarbon. Note that the SuSAv2 2p2h and GENIE pion absorption contributions are added to each model for comparison with the data.

1. *Carbon and Oxygen*

Fig. 4 shows the T2K ν_μ CC0π cross-section measurement on carbon compared to HF-CRPA predictions, including the additional 2p2h and pion absorption contributions, split by interaction mode whilst Fig. 5 shows a comparison of all the considered GENIE models to the full carbon and oxygen measurement.

It can be noted that all the models are in excellent agreement with each other and reasonable agreement with the T2K measurement at large angles ($\cos\theta_\mu$<0.6), which corresponds to regions of large q_0 and q_3. In this region the cross section is driven mostly by nucleon level physics, related to the choice of form factors which are very similar for all the considered models (all use a dipole axial form factor with a nucleon axial mass close to 1 GeV). At more forward angles (and therefore correspondingly lower q_0, q_3) nuclear effects become more important and the models begin to differ. As discussed in the context of Fig. 3, it's clear how RPA has a large impact even at intermediate angles (0.6<$\cos\theta_\mu$<0.86). The largest model differences are seen in the very forward region, where the treatment of FSI effects in HF(-CRPA) and deviations from the impulse approximation are most important. In the most forward regions, no model can describe the data for the oxygen cross section whilst only the strong suppression from RPA can describe the carbon results. However, it is clear from Fig. 4 that the poor agreement between HF-CRPA and the data may be due to the mismodelling of interaction modes beyond CCQE. Future exclusive analyses, such as those preliminarily presented by the MINERvA collaboration in Ref. [35], may be able to use outgoing nucleon kinematics to determine whether the over-prediction of the data at forward angles is concentrated at kinematics best matching CCQE or other interaction channels.

Fig. 6 shows the prediction of the carbon to oxygen and argon cross section ratios predicted by each model, demonstrating substantial differences. It can be noted that HF(-CRPA) predicts that the cross section for oxygen may be lower compared to that of carbon at forward angles (and so at low q_0, q_3), as hinted by the T2K measurement (but with large uncertainties), whilst the ratios from the other models remain almost flat. This

oxygen-carbon difference remains for HF with and without CRPA corrections and was previously shown for cross sections at fixed incoming energy [36]. Since oxygen is a double magic nucleus, this lower cross section at forward angles can be expected. As carbon and oxygen tend to have quite similar initial-state properties in the HF (e.g. binding energies and momentum distributions), this effect might be obscured in a factorised PWIA approach while it is present with a consistent treatment of initial- and final-state wavefunctions. For the carbon to argon ratio an even larger difference is seen between the models, where it appears that CRPA has a large impact on the cross section ratio, especially at forward angles, but that RPA effects do not.

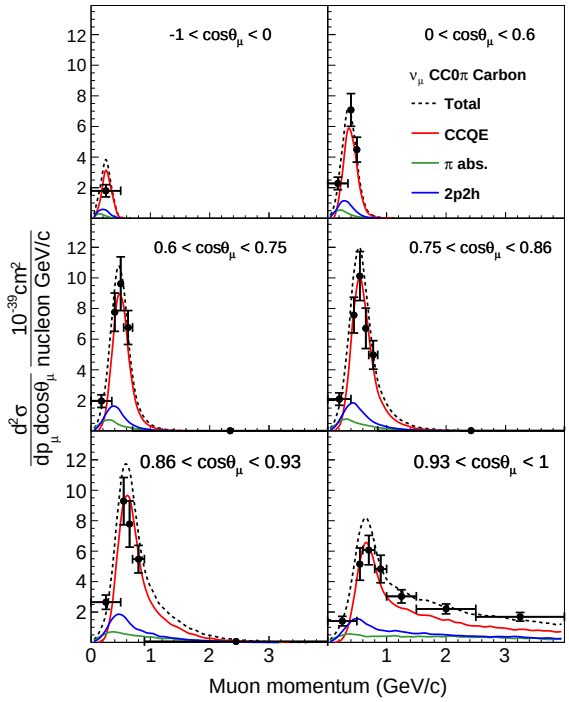

FIG. 4. The T2K flux-integrated CC0π ν_μ double differential cross section on carbon as a function of outgoing muon kinematics as predicted by the newly implemented HF-CRPA model compared to T2K measurements [18]. The prediction is split by interaction mode. Note that the new implementation is only the CCQE contribution, the non-CCQE contributions are described in Sec I.

2. *Neutrino and anti-neutrino*

Fig. 7 shows the T2K $\bar{\nu}_\mu$ CC0π cross-section measurement on hydrocarbon compared to HF-CRPA predictions split by interaction mode whilst Fig. 8 shows a comparison of all the considered GENIE models to the full T2K neutrino and anti-neutrino measurement. It can be seen that for anti-neutrino interactions the hydrogen contribution (which is extremely similar between all models) is particularly significant at forward angles, where it is not subject to the same suppression from nuclear effects as the carbon contribution. As in the carbon and oxygen case, the models differ most significantly at forward angles. It can further be seen that the reduction of the cross section for anti-neutrino interactions in the most forward angular slice with respect to the penultimate slice is much stronger for HF(-CRPA) than for LFG(+RPA). It can also be seen how the impact of RPA is much stronger than CRPA for both neutrinos and anti-neutrinos. RPA corrections tend to be stronger for neutrino than for anti-neutrino, whilst CRPA shows more similar strength.

It is clear that all models significantly overestimate the T2K anti-neutrino measurement at forward angles, with possible the exception of HF-CRPA in the most forward slice, and all models other than LFG-RPA struggle to describe the neutrino measurement. Whilst it is once again tempting to interpret this as a requirement for a strong RPA-like CCQE suppression, the non-negligible contributions from nonQE interaction modes allows an alternative resolution by a significant reduction of the pion absorption and 2p2h strengths.

IV. DISCUSSION AND CONCLUSIONS

The demonstrated differences in model predictions for the evolution of the cross section as a function of neutrino energy, kinematics, flavour and target can imply challenges for near-to-far detector extrapolation for neutrino oscillation analyses. For example, it is clear from Fig. 2 and 3 that the impact of nucleon correlations influences the shape of both the total and differential cross section differently for the RPA and CRPA approaches. This implies that constraints from a near detector may be incorrectly propagated to the far detector if nucleon correlations are mis-modelled. Similarly Fig 5 and 6 shows that the extrapolation of cross sections from one target to another is quite dependent on the model used, especially in regions of low q_0, q_3. Taking the spread of the model predictions as a minimum gauge of current uncertainty would suggest that the cross section ratio between different nuclear targets may not be controlled at better than the 5%-10% level. As stated in Sec III A, Fig. 7 additionally demonstrates significant differences in the prediction for neutrino and anti-neutrino differences between models, also most notably at low q_0, q_3. A mismodelling of such differences can bias extrapolations of constraints from neutrino to anti-neutrino interactions from typically neutrino-dominant near detector data, potentially affecting measurements of CPV.

It is clear from Tab I that none of the models tested are able to describe the complete T2K measurements, typically due to overestimates of the cross section at forward angles ($\cos\theta_\mu$>0.8). The strong suppression from RPA seems to be favoured in the carbon and oxygen analysis although, as noted in Sec III A, it's possible a similar reduction could be obtained by reducing the non-CCQE

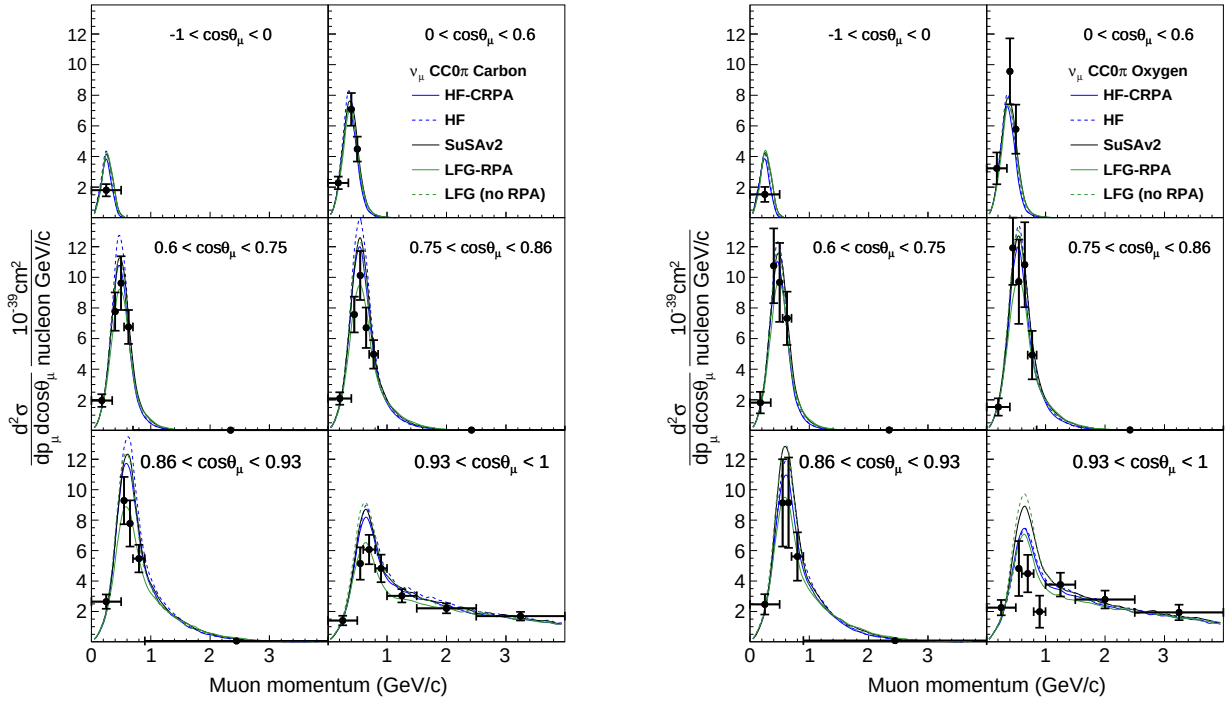

FIG. 5. The T2K flux-integrated CC0π ν_μ double differential cross section on carbon and oxygen as a function of outgoing muon kinematics predicted by various models compared to T2K measurements [18]. Note that the new implementation is only the CCQE contribution, the non-CCQE contributions are described in Sec I.

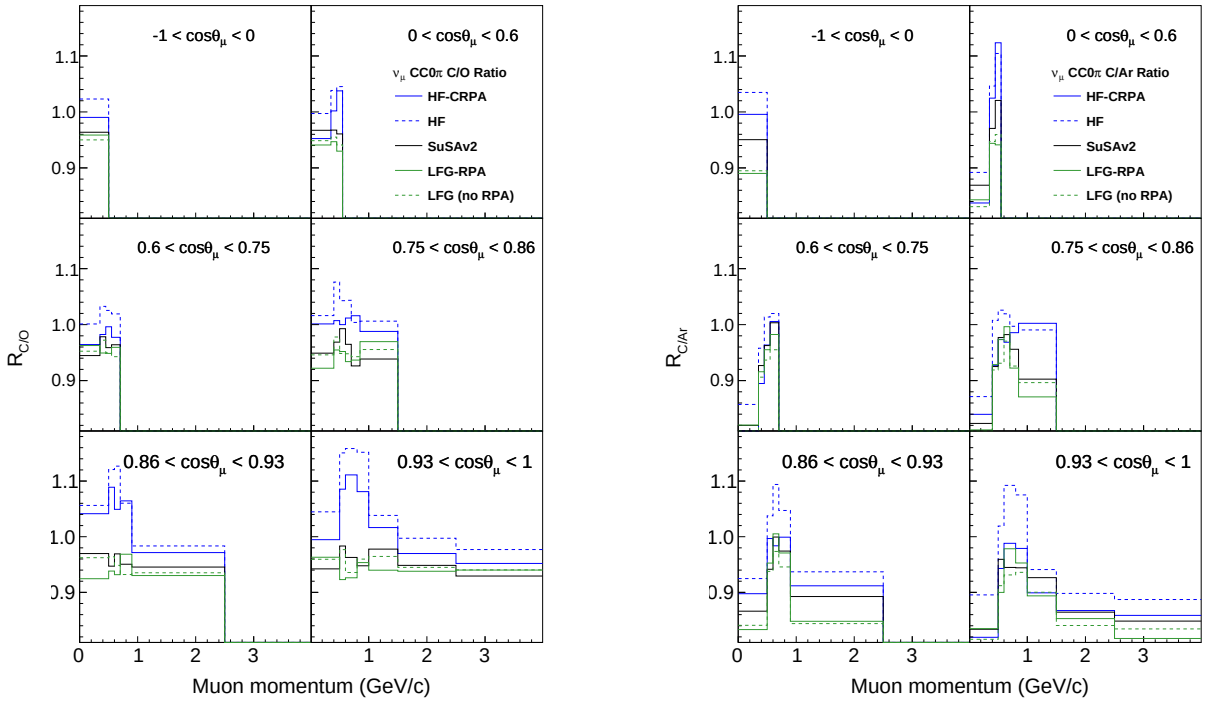

FIG. 6. The T2K flux-integrated CC0π ν_μ double differential cross section ratio between carbon and oxygen (left) or argon (right) as predicted by various models. Bins in which the cross section is too small for a meaningful ratio to be calculated are left empty. Note that the new implementation is only the CCQE contribution, the non-CCQE contributions are described in Sec I.

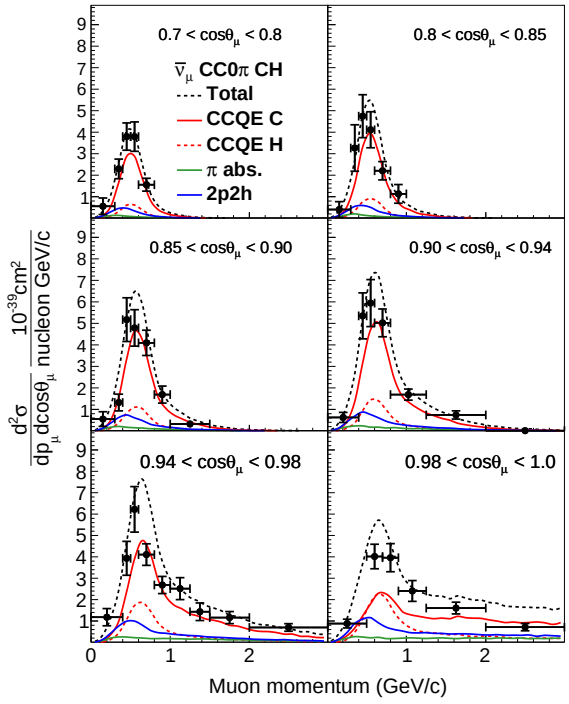

FIG. 7. The T2K flux-integrated CC0π $\bar{\nu}_\mu$ double differential cross section on hydrocarbon (CH) as a function of outgoing muon kinematics as predicted by the newly implemented HF-CRPA model compared to T2K measurements [19]. The prediction is split by interaction mode and, for the CCQE case, into whether the interaction is with a carbon or hydrogen target nucleus. Note that the new implementation is only the CCQE contribution, the non-CCQE contributions are described in Sec I.

contributions. With this in mind, it is interesting to note the observation that the SuSAv2-MEC model for 2p2h interactions predicts a stronger contribution at forward angles compared to alternative models such as the GFMC calculation [37], while providing a similar result for the more backward bins (see Ref. [26] for a more detailed discussion).

Overall the HF-CRPA model predicts that approximately 15% (17%) of CCQE events in the T2K electron (muon) neutrino flux after oscillations are within the challenging low q_0, q_3 region where model differences are strongest (taking it to be broadly characterised by q_3 <300 MeV/c, q_0 <50 MeV). It is therefore clear that as experiments gather more statistics, an accurate modelling of this region is required, alongside a cautious assignment of associated systematic uncertainties.

In conclusion, the HF and HF-CRPA models have been implemented in GENIE and give substantially different predictions from other available models, particularly at low momentum and energy transfer. It has further been shown that the predicted evolution of the cross section as a function of neutrino energy, kinematics, flavour and target all differ between the newly implemented models and the other GENIE models considered. Since neutrino oscillation measurements typically rely on the correct modelling of at least some aspects of this evolution when extrapolating constraints from a near detector to a far detector, the addition of the HF(-CRPA) models to GENIE provide an important means to evaluate potential systematic uncertainties within future analyses.

ACKNOWLEDGEMENTS

The authors would like to thank the GENIE collaboration and all the HF-CRPA model authors from the Ghent University group. SD is particularly grateful for fruitful conversations with Steve Dytman and technical help from Marco Roda. VP acknowledges the support from US DOE under grant DE-SC0009824. This manuscript has been authored by Fermi Research Alliance, LLC under Contract No. DE-AC02-07CH11359 with the U.S. Department of Energy, Office of Science, Office of High Energy Physics. The project was realised thanks to the CERN summer student program, which supported OP.

Appendix A: Implementation validations

The model implementation was validated to accurately reproduce both the hadron tensor elements as a function of q_0, q_3 and the complete double differential cross section for a variety of fixed incoming neutrino energies. An example set of validations is shown in Fig. 9, which demonstrates a comparison of the HF-CRPA theory code and the GENIE implementation calculation of the double differential cross section on a carbon target. It can be seen that the agreement is near-perfect, with the small differences stemming from details of interpolation methods and the fact the GENIE event calculation requires a finite sized angular range in which to select events to calculate the cross section (Fig. 9 plot uses a 0.02 range of $\cos\theta_\mu$).

[1] K. Abe *et al.* (T2K), Nucl. Instrum. Meth. A **659**, 106 (2011), arXiv:1106.1238 [physics.ins-det].
[2] D. S. Ayres *et al.* (NOvA), (2007), 10.2172/935497.
[3] K. Abe *et al.* (Hyper-Kamiokande), (2018), arXiv:1805.04163 [physics.ins-det].
[4] B. Abi *et al.* (DUNE), (2020), arXiv:2002.03005 [hep-ex].
[5] L. Alvarez-Ruso *et al.*, Prog. Part. Nucl. Phys. **100**, 1 (2018), arXiv:1706.03621 [hep-ph].
[6] N. Jachowicz, K. Heyde, J. Ryckebusch, and S. Rombouts, Phys. Rev. C **65**, 025501 (2002).

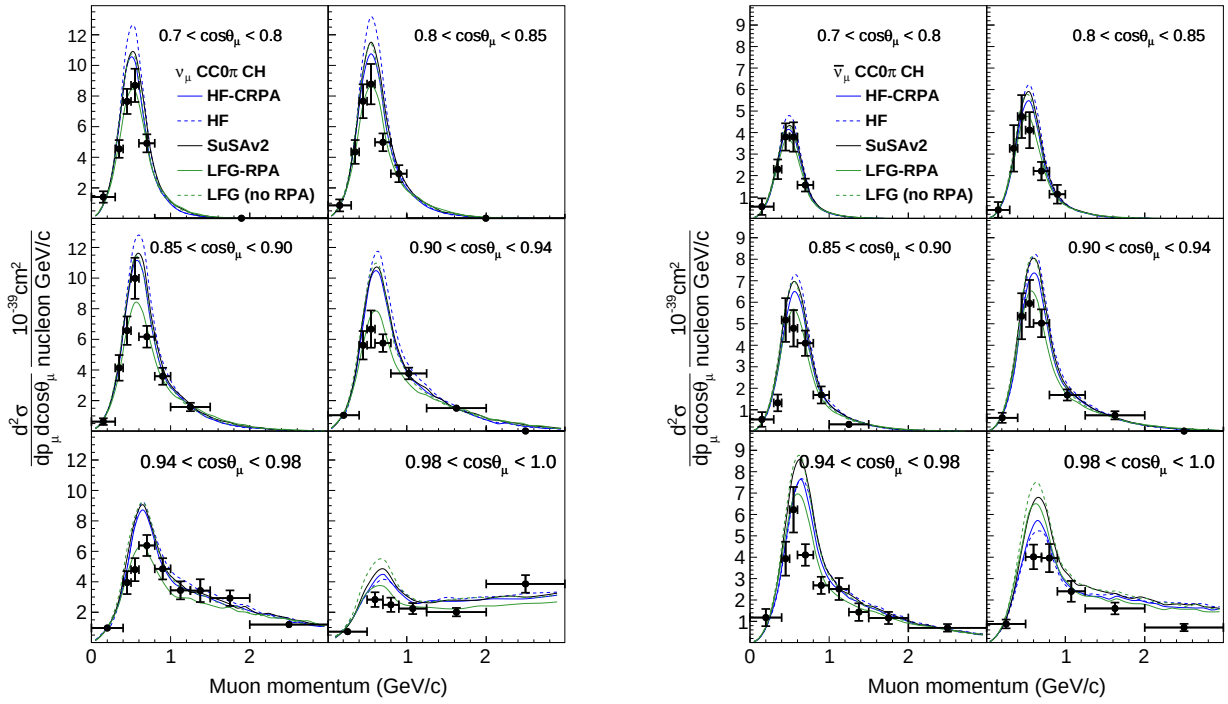

FIG. 8. The T2K flux-integrated CC0π ν_μ and $\bar{\nu}_\mu$ double differential cross section on carbon and oxygen as a function of outgoing muon kinematics predicted by various models compared to T2K measurements [19]. Note that the new implementation is only the CCQE contribution, the non-CCQE contributions are described in Sec I.

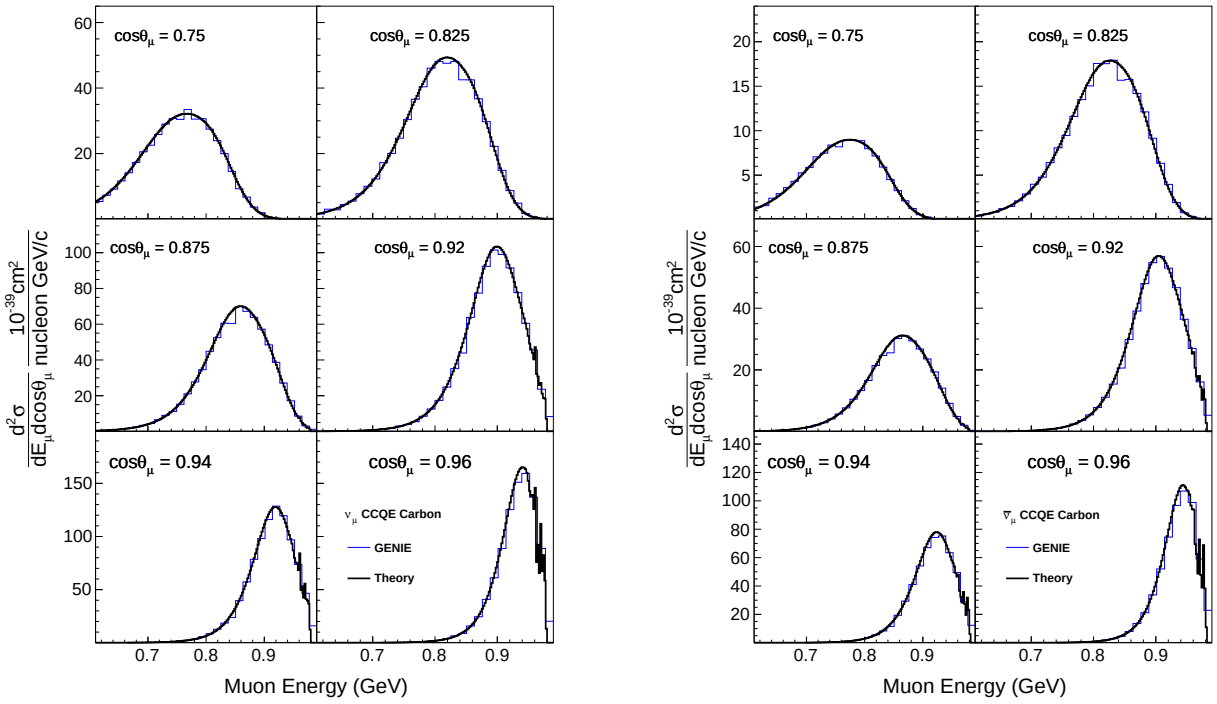

FIG. 9. The double differential cross section from the HF-CRPA theory code and the GENIE implementation are shown for neutrino (left) and anti-neutrino (right) CCQE interaction on a carbon target with a fixed 1 GeV incoming muon neutrino energy.

[7] V. Pandey, N. Jachowicz, T. Van Cuyck, J. Ryckebusch, and M. Martini, Phys. Rev. C **92**, 024606 (2015), arXiv:1412.4624 [nucl-th].

[8] A. Nikolakopoulos, M. Martini, M. Ericson, N. Van Dessel, R. González-Jiménez, and N. Jachowicz, Phys. Rev. C **98**, 054603 (2018), arXiv:1808.07520 [nucl-th].

[9] J. Ryckebusch, M. Waroquier, K. Heyde, J. Moreau, and D. Ryckbosch, Nuclear Physics A **476**, 237 (1988).

[10] J. Ryckebusch, K. Heyde, D. Van Neck, and M. Waroquier, Nuclear Physics A **503**, 694 (1989).

[11] A. Nikolakopoulos, N. Jachowicz, N. Van Dessel, K. Niewczas, R. González-Jiménez, J. M. Udías, and V. Pandey, Phys. Rev. Lett. **123**, 052501 (2019), arXiv:1901.08050 [nucl-th].

[12] C. Andreopoulos *et al.*, Nucl. Instrum. Meth. **A614**, 87 (2010), arXiv:0905.2517 [hep-ph].

[13] C. Andreopoulos, C. Barry, S. Dytman, H. Gallagher, T. Golan, R. Hatcher, G. Perdue, and J. Yarba, (2015), arXiv:1510.05494 [hep-ph].

[14] R. González-Jiménez, G. D. Megias, M. B. Barbaro, J. A. Caballero, and T. W. Donnelly, Phys. Rev. **C90**, 035501 (2014), arXiv:1407.8346 [nucl-th].

[15] G. D. Megias, J. E. Amaro, M. B. Barbaro, J. A. Caballero, and T. W. Donnelly, Phys. Rev. **D94**, 013012 (2016), arXiv:1603.08396 [nucl-th].

[16] S. Dolan, G. D. Megias, and S. Bolognesi, Phys. Rev. D **101**, 033003 (2020), arXiv:1905.08556 [hep-ex].

[17] J. Nieves, I. Ruiz Simo, and M. J. Vicente Vacas, Phys. Rev. **C83**, 045501 (2011), arXiv:1102.2777 [hep-ph].

[18] K. Abe *et al.* (T2K), Phys. Rev. D **101**, 112004 (2020), arXiv:2004.05434 [hep-ex].

[19] K. Abe *et al.* (T2K), Phys. Rev. D **101**, 112001 (2020), arXiv:2002.09323 [hep-ex].

[20] I. Ruiz Simo, J. E. Amaro, M. B. Barbaro, A. De Pace, J. A. Caballero, and T. W. Donnelly, J. Phys. G **44**, 065105 (2017), arXiv:1604.08423 [nucl-th].

[21] I. Ruiz Simo, J. E. Amaro, M. B. Barbaro, A. De Pace, J. A. Caballero, G. D. Megias, and T. W. Donnelly, Phys. Lett. **B762**, 124 (2016), arXiv:1607.08451 [nucl-th].

[22] C. Berger and L. M. Sehgal, Phys. Rev. D **76**, 113004 (2007).

[23] S. Dytman, Y. Hayato, R. Raboanary, J. T. Sobczyk, J. Tena Vidal, and N. Vololoniaina, Phys. Rev. D **104**, 053006 (2021), arXiv:2103.07535 [hep-ph].

[24] K. Niewczas, A. Nikolakopoulos, J. T. Sobczyk, N. Jachowicz, and R. González-Jiménez, Phys. Rev. D **103**, 053003 (2021), arXiv:2011.05269 [hep-ph].

[25] J. Schwehr, D. Cherdack, and R. Gran, (2017), arXiv:1601.02038 [hep-ph].

[26] N. Jachowicz and A. Nikolakopoulos, (2021), arXiv:2110.11321 [nucl-th].

[27] J. E. Amaro, M. B. Barbaro, J. A. Caballero, T. W. Donnelly, A. Molinari, and I. Sick, Phys. Rev. **C71**, 015501 (2005), arXiv:nucl-th/0409078 [nucl-th].

[28] G. D. Megias, *Charged-current neutrino interactions with nucleons and nuclei at intermediate energies*, Ph.D. thesis, University of Seville, Spain (2017), https://idus.us.es/xmlui/handle/11441/74826.

[29] R. González-Jiménez, M. B. Barbaro, J. A. Caballero, T. W. Donnelly, N. Jachowicz, G. D. Megias, K. Niewczas, A. Nikolakopoulos, and J. M. Udías, Phys. Rev. C **101**, 015503 (2020), arXiv:1909.07497 [nucl-th].

[30] G. D. Megias, J. E. Amaro, M. B. Barbaro, J. A. Caballero, and T. W. Donnelly, Phys. Rev. D **94**, 013012 (2016).

[31] K. Abe *et al.* (T2K), Phys. Rev. **D87**, 012001 (2013), [Addendum: Phys. Rev.D87,no.1,019902(2013)], arXiv:1211.0469 [hep-ex].

[32] `http://t2k-experiment.org/wp-content/uploads/T2Kflux2016.tar`, accessed: 2019-08-07.

[33] M. Martini, N. Jachowicz, M. Ericson, V. Pandey, T. Van Cuyck, and N. Van Dessel, Phys. Rev. C **94**, 015501 (2016), arXiv:1602.00230 [nucl-th].

[34] A. Nikolakopoulos, V. Pandey, J. Spitz, and N. Jachowicz, Phys. Rev. C **103**, 064603 (2021), arXiv:2010.05794 [nucl-th].

[35] D. Ruterbories for the MINERvA collaboration, "The most elastic interactions of neutrinos at minerva: The recoil strikes back," URL: `https://theory.fnal.gov/events/event/results-from-minerva-8/` (2019).

[36] N. Van Dessel, N. Jachowicz, R. González-Jiménez, V. Pandey, and T. Van Cuyck, Phys. Rev. C **97**, 044616 (2018), arXiv:1704.07817 [nucl-th].

[37] A. Lovato, J. Carlson, S. Gandolfi, N. Rocco, and R. Schiavilla, Phys. Rev. X **10**, 031068 (2020).